scientific reports

OPEN

Self-propelled directed transport of C60 fullerene on the surface of the cone-shaped carbon nanotubes

Mehran Vaezi[1] & Hossein Nejat Pishkenari[2✉]

Directed transportation of materials at molecular scale is important due to its crucial role in the development of nanoelectromechanical devices, particularly the directional movements along the carbon nanotubes (CNTs), due to the applications of CNTs as nano-manipulators, confined reactors, and drug or other materials delivery systems. In the present investigation, we evaluate the movements of C60 fullerenes on the surface of the cone-shaped CNTs. The fullerene molecules indicate directed motion toward the narrower end of CNTs, which is due to the potential energy gradient along the nanotube length. A continuum model is proposed to evaluate the mechanism of the directed motion and the results of the theoretical model are compared with numerical simulations. Directed movements have been examined at various opening angles of CNTs, considering the trajectories of motions, variation of potential energy, and diffusion coefficients. At smaller opening angles, the driving force on the C60 increases and the molecule experiences more directed transport along the nanotube. The motion of fullerene has also been simulated inside the cone-shaped CNTs, with similar opening angle, and different average radius. At lower average radius of the cone-like nanotubes, the motion of C60 is comparatively more rectilinear. Directional transport of fullerene has been observed in the opposite direction, when the molecule moves on the external surface of the cone-like CNTs, which is due to the stronger interaction of C60 with the parts of the external surface with larger radius. The effect of temperature has been evaluated by performing the simulations at the temperature range of 100 to 400 K. The direction of the velocity reveals that the thermal fluctuations at higher temperatures hinder the directed motion of molecule along the cone-shaped CNTs. The results of the present study propose a new method to obtain directed transport of molecules which can be helpful in different applications such as drug delivery systems.

Achieving directed motion at nano-scale has a crucial role for several applications in the field of nanotechnology[1,2]. Manufacturing functional nano-devices through the directed assembly of smaller nanoparticles[3], is among the applications of controlling the movements of low-dimensional materials. Steered locomotion of nanostructures can also be exploited to perform precise tasks at molecular dimensions[4]. As an instance, Regan et al.[5] reported the fabrication of a mass conveyor based on carbon nanotubes, or Barreiro and her colleagues[6] could transport the gold particle cargoes with sub-nanometer accuracy along the nanotube length.

Controlling the molecular motions along the nanotube is of particular importance, due to the special applications of this nanostructure. Due to the hollow structure of nanotubes, they are employed as nano-reactors[7–9], in which several products can be achieved. Kuzmany et al.[10] synthesized sub-nanometer graphene nano-ribbons by the reactions of ferrocene molecules inside the carbon nanotubes. The reaction of fullerene molecules has been studied inside the CNT, as well. At elevated temperatures, C60 fullerenes transform into different products in carbon nanotube such as inner nanotube[11], and C60 oligomers and polymers[12]. Consequently, controllable transport of materials inside the CNT can help to control the kinetics of the reactions confined within the nanotubes. Moreover, carbon nanotubes have shown considerable potential as the atomic force microscope tips[13–15]. As a result, controlling the maneuverability of particles on the CNT can provide the opportunity to design precise nano-manipulators[16,17].

Directional motion at molecular scale has been reported in previous investigations[18–21], using various techniques. Rectilinear transport of materials has been obtained on the surfaces subjected to strain gradient[22–25], on which adsorbed molecules move from regions with higher strain to less strained parts[26]. Constructing vacancies on the surface is another method to direct the motion of adsorbed materials[27]. Youzi et al.[28]

[1]Center for Nanoscience and Nanotechnology, Institute for Convergence Science and Technology, Sharif University of Technology, Tehran 14588-89694, Iran. [2]Nano Robotics Laboratory, Mechanical Engineering Department, Sharif University of Technology, Tehran, Iran. ✉email:

demonstrated the one-dimensional motion of molecular machines, surrounded by the series of vacancies, on the silicene surface. Applying temperature gradient on the substrate is another technique to steer the molecular motions[29]. The adsorbed materials migrate to the lower temperature area, due to the lower free energy level in these regions[30]. The nanoscale directed movement has also been obtained by angustotaxis effect[31], where a trapped capped nanotube is derived toward the narrower end of a channel. The underlying physics is attributed to the higher contact area between the nanotube and the channel, at narrower side.

Several attempts were made so far to control the motion of nanoparticles along the carbon nanotubes. Previous studies reported the fabrication of artificial nanomotor consists of a short CNT which can translate relative to a coaxial inner longer nanotube[6]. The electric voltage applied to the ends of longer nanotube leads to a temperature gradient along the CNT. The shorter nanotube prefers to move toward the ends of longer CNT which have a lower temperature. The electromigration phenomenon has also been employed for achieving reversible mass transport along the carbon nanotubes[5]. By establishing electric current through the carbon nanotube, the indium nanoparticles experience directed movements on the external surface of the nanotube. The migration of the electrons can move indium particles through the collisions and momentum transfer. Using molecular dynamics simulations, Legoas et al.[32] showed the presence of a retraction force on the extruded core of a double-walled carbon nanotube. After the release of extruded core, it is completely retracted inside the outer shell. The retraction force is due to the increase of contact area between the core and the outer shell. Machado and the colleagues[33] reported the curvature driven motion of the encapsulated CNT inside a spiral-shaped carbon nanotube. Since the bending energy of the inner nanotube is proportional to the square of curvature, the encapsulated CNT experiences a driving force toward the regions of lower curvature. Despite proposing different techniques for nano-manipulations along the CNTs, using cone-shaped nanotubes did not receive attention in the previous investigations. The conical carbon nanotubes are experimentally synthesized through different methods such as arc discharge[34], vapor deposition[35], pyrolysis[36] and bottom-up organic synthesis[37,38]. Exploiting conical nanotubes for controlling the movements seems more practical than the previous methods such as using a spiral-shaped CNT or an extruded core of the double-walled nanotube.

In the present study, we investigate the directed transport of fullerene molecule along the cone-like carbon nanotubes. Directed motions of C60 fullerenes are studied inside the CNTs with different opening angles. For this purpose, we consider the trajectories of motion, variation of the potential energy, potential energy surface (PES) analysis, and the diffusion coefficients. A continuum model has been proposed to evaluate the mechanism of the directed motion. At a similar opening angle of the cone-like CNTs, we evaluate the effect of average radius, by calculating the distribution of the fullerene velocity, and the trajectories of motion. The transportation of molecules has also been studied outside the nanotubes. In case of moving outside the cone-shaped nanotube, the fullerene molecule shows directed motion in opposite direction compared with the motion inside the CNT. Ultimately, we consider the effect of temperature on the directionality of the motion.

Computational methods

The motion of C60 fullerene has been simulated on the surface of the cone-like CNTs, using an all-atom molecular dynamics method. The fullerene molecule moves inside/outside the nanotubes, with different opening angles, as illustrated in Fig. 1. The radius of the CNTs decreases linearly along their length. Different cone angles (hereafter called as α angle) have been chosen including 112.9, 60.0, and 19.2 degrees, while the slant length of CNTs is 80Å. The atomic structures of the carbon nanotube were obtained from Nanotube Modeler[39]. The fullerene nanostructure contains 60 sp^2 carbon atoms, arranged in 20 hexagonal and 12 pentagonal faces[40].

Different simulations have been performed in the canonical NVT ensemble, which was implemented by the Nose-Hoover thermostat[41,42]. The temperature of the simulations was set to 100 K, and the damping parameter of the thermostats was 100 fs. It should be mentioned that, in Sect. 3.4, where we evaluate the effect of temperature, the temperature of the system changes from 100 K to 400 K. The inter-molecular interactions of C60 and nanotubes were described by Lennard-Jones (LJ) potential, $\varphi = 4\epsilon \left(\left(\frac{\sigma}{l} \right)^{12} - \left(\frac{\sigma}{l} \right)^{6} \right)$. When the distance between a pair of atoms (l) is equal to $2^{1/6}\sigma$, the atoms find the minimum potential energy of ϵ. In our simulations, ϵ and σ parameters were assumed, 2.4 meV and 3.4Å, respectively[43]; which is suitable for describing the interactions between carbon atoms[44]. The cut-off radius of the pair potential was considered 12 Å. The inner-interactions of C60 atoms were captured by Tersoff potential[45]. To understand the effect of CNTs characteristics on the transportation more precisely, the nanotubes had fixed structures during the simulations.

The fullerene molecule was initially placed on the top part of CNTs with the largest radius (red region in Fig. 1), and the potential energy was minimized to find its local stable position. The initial velocity of C60 fullerene corresponds to the temperature of the simulation systems. The reproducibility of the results was examined by repeating the simulations, at different initial conditions of C60 (i.e., different distribution of the initial velocity). All of the simulations were conducted by Large-scale Atomic/Molecular Massively Parallel Simulator (i.e., LAMMPS package)[46]. The equations of the motions were integrated by velocity Verlet method[47], and the time step of the integrations was adjusted to 1 fs. Each simulation continued until the C60 reached the narrower part of the CNT (blue parts in Fig. 1).

Results and discussion
### Mechanism of the motion: Continuum approach and numerical simulations

To understand the mechanism of the directed motion of C60, the analysis of the potential energy has been performed. In this analysis, the fullerene molecule is translated to different points in horizontal plane (x-y plane). At each horizontal position (e.g., (x_0, y_0)), the molecule is displaced to different heights along the z-axis. The potential energy between C60 and carbon nanotube is calculated at each height, and the minimum potential energy of the molecule is captured. It should be noted that, the translation of C60 occurs with the step-
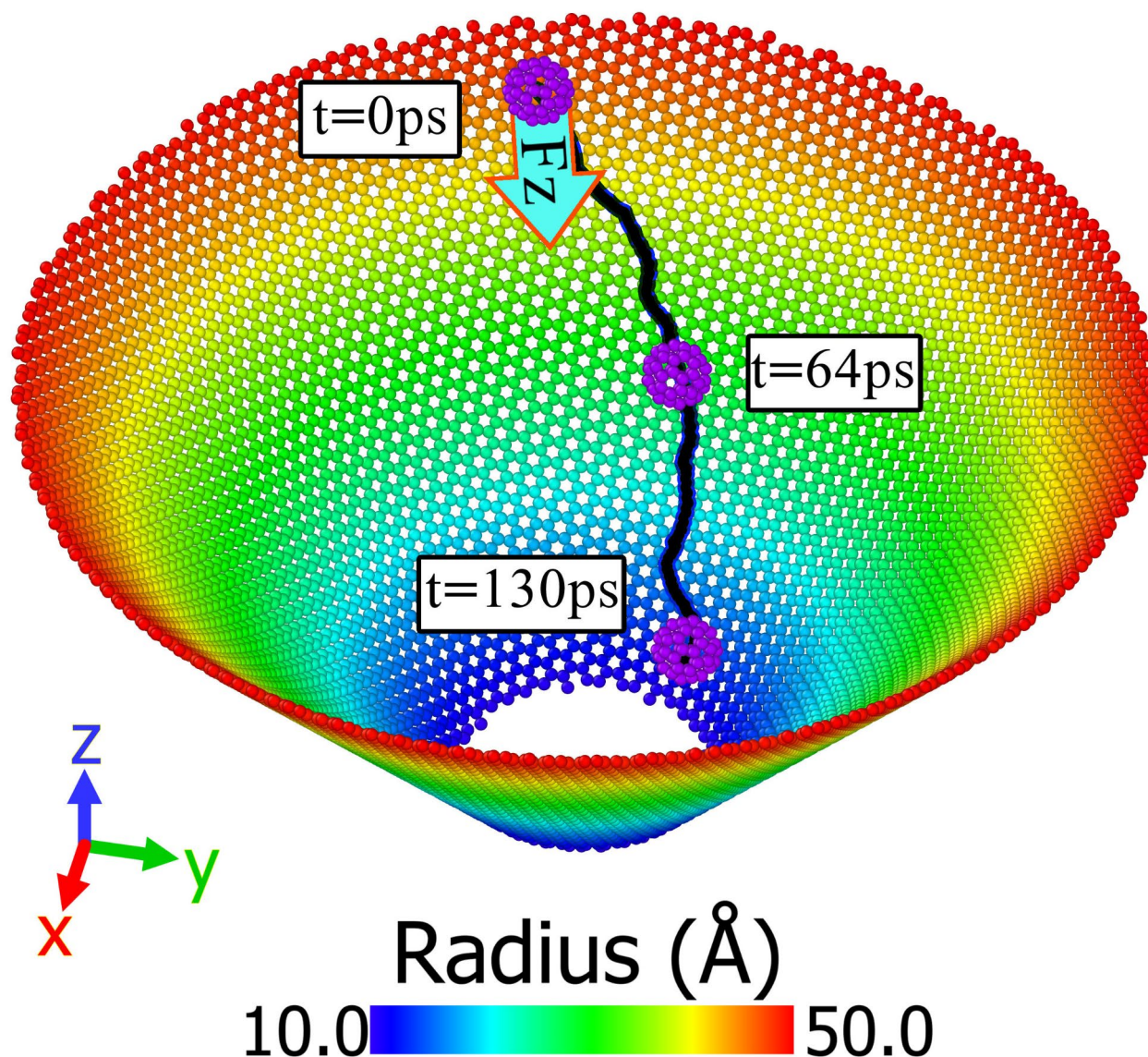
Fig. 1. One of the cone-shaped nanotubes used in the simulations. The slant length of the nanotube is 80 Å, and the opening angle is 60.0 degrees. The color bar indicates the variations of the CNT radius. The axes of nanotubes are parallel to the z-axis of the coordinate system.

length of 0.5 Å in the directions of x-, y-, and z-axis, and the nanotube has the opening angle of 38.9 degrees. Figure 2 shows the results of the analysis of potential energy. Based on this analysis, as we move from the wider end of the CNT ($R_{\max}$) to the narrower end ($R_{\min}$), the reduction of the potential energy is observed. The potential energy gradient along the length of CNT provides the driving force on the fullerene. Hence, the C60 molecule demonstrates directed motion inside the nanotube. At the wider end of the CNT, the potential energy of fullerene is almost -0.6 eV, which is similar to the case where the C60 is on a graphene surface[48]. The potential energy level decreases to -1.1 eV, at the narrower end of the CNT, which is approximately equal to the potential energy of a C60, sandwiched between two graphene layers. Since the fullerene is more stable at the narrower end of the CNT, it experiences a directed movement along the cone-like nanotubes.

The variation of the potential energy of C60 has been analyzed, using a continuum model. The continuum model is indeed a valuable tool for predicting the interactions between the materials. The continuum model assumes that matter is continuous and completely fills the space it occupies, while the materials consist of discrete atoms. In the present study, the surface of the nanotubes is considered continuous. This assumption is true if the materials include a large number of atoms. In case of nanomaterials with few number of atoms the continuous assumption is not right. Here, since the conical nanotubes contain thousands of atoms we are allowed to use the assumption. Considering a discrete structure for the surface of nanotubes, we should calculate the summation of the vdW interactions between the adsorbed atom (an atom of fullerene) and all of the atoms
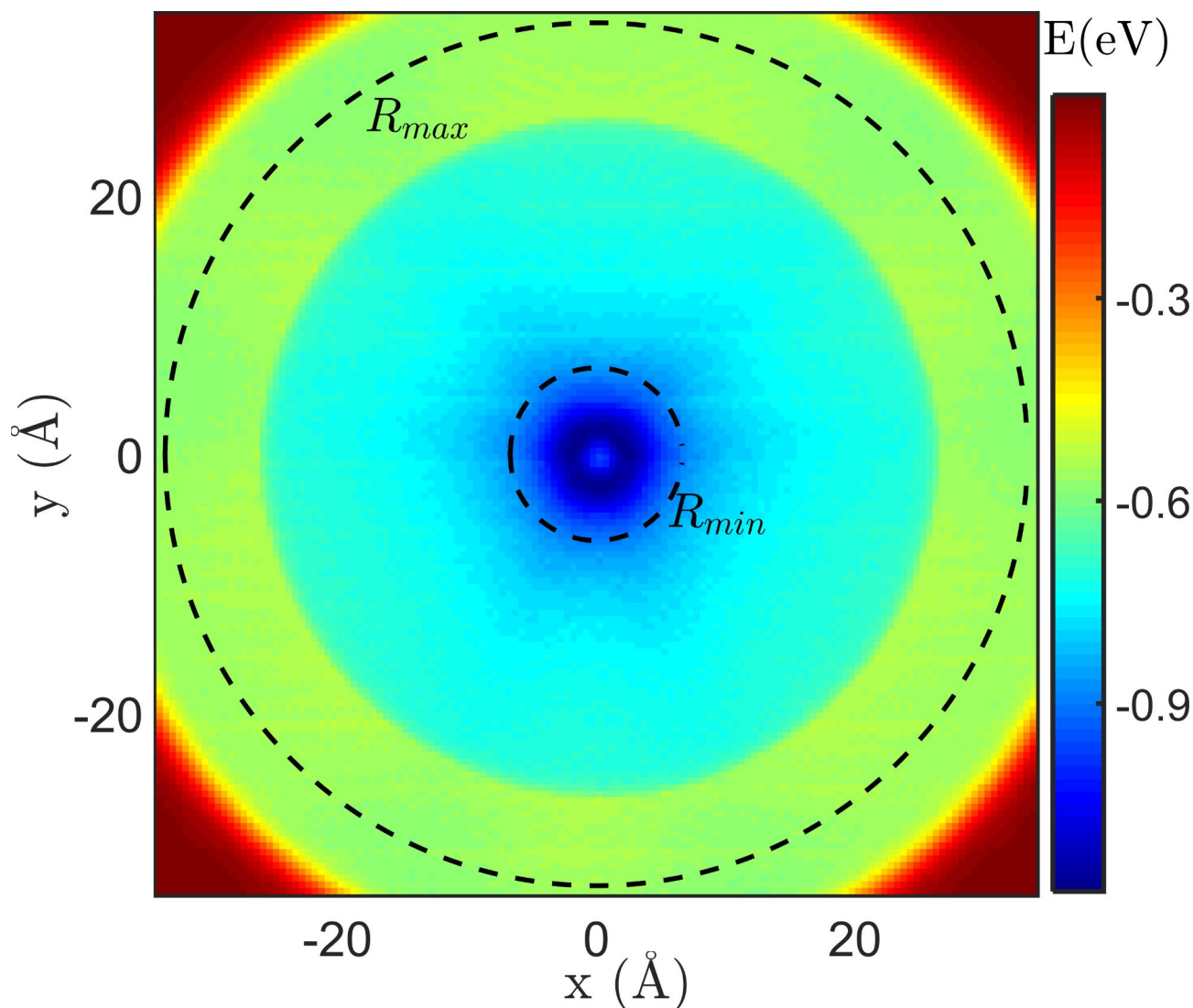
Fig. 2. Analysis of the potential energy of C60. At each horizontal position such as (x_0, y_0), we displaced the C60 in the direction of z-axis, and the minimum energy has been captured which is corresponding to a specific height of molecule (e.g., z_0).

of the cone-shaped CNT. On the other hand, when we use continuum model, the interaction of adsorbed atom and nanotube is obtained by calculating an integral over the surface of the cone-shaped CNT. As a result, the computational costs decrease as the continuum model is employed. However, the continuum model may lead to the complex integrals which should be solved by the numerical methods.

As mentioned in the model, it is assumed that the carbon atoms are uniformly distributed on the surface of the cone-shaped CNT. As a result, the potential energy between an adsorbed atom (an atom of C60) and CNT is calculated by integrating the Lennard-Jones potential as follows,

$$U_{adatom} = \iint \varphi(r, \theta, z) \, \rho_A \frac{1}{\sin\alpha/2} r dr d\theta . \tag{1}$$

In the recent equation, φ is the LJ potential energy which is a function of the coordinates of CNT's atoms (i.e., (r, θ, z)), ρ_A is the areal density of the atoms over the CNT surface, and $\frac{1}{\sin\alpha/2} r dr d\theta$ is surface element of a cone-like CNT with the opening angle of α. The 6–12 Lennard-Jones potential function is given by

$$\varphi = 4\epsilon \left(\left(\frac{\sigma}{l}\right)^{12} - \left(\frac{\sigma}{l}\right)^{6} \right) \tag{2}$$

where, ϵ and σ are the LJ parameters and l is the distance between the adatom and the surface element of CNT. Considering the position of adatom as (r_0, θ_0, z_0) and the position of the surface element as (r, θ, z), the separation distance can be written as,

$$l^2 = r^2 + r_0^2 - 2rr_0\cos(\theta - \theta_0) + (z - z_0)^2. \tag{3}$$

By substituting Eq. 7 into Eq. 1, the potential energy between adatom and con-like surface is rewritten as,

$$U_{adatom} = U_R - U_A \tag{4}$$

where, U_R and U_A are expressed as,

$$U_R = \frac{4\epsilon \rho_A \sigma^{12}}{\sin(\alpha/2)} \int_0^{2\pi} \int_{R_{min}}^{R_{max}} \frac{rdrd\theta}{\left[r^2 + r_0^2 - 2rr_0\cos(\theta - \theta_0) + (rcot(\alpha/2) - z_0)^2\right]^6}$$

$$U_A = \frac{4\epsilon \rho_A \sigma^{6}}{\sin(\alpha/2)} \int_0^{2\pi} \int_{R_{min}}^{R_{max}} \frac{rdrd\theta}{\left[r^2 + r_0^2 - 2rr_0\cos(\theta - \theta_0) + (rcot(\alpha/2) - z_0)^2\right]^3}. \tag{5}$$

The cone equation in cylindrical coordinate is considered as $z = rcot(\alpha/2)$, and the apex of the cone-like CNT is located at the origin of the coordinate system as shown in Fig. 3d. The total potential energy between C60 and cone-shaped CNT is calculated by adding up the potential energies of all atoms in the C60 molecule.

$$U_{total} = \sum_{i=1}^{60} U_R(i) - U_A(i) \tag{6}$$

In the next step, the C60 was displaced along the nanotube length, while the molecule is located in equilibrium distance to the CNT wall. The trajectory of the translation of C60 inside the nanotube is demonstrated in Fig. 3d. At each position of C60 inside the cone-like CNT, we calculate the potential energy of molecule (U_{total}) by numerical integration of the Eq. 5. Figure 3 demonstrates the potential energy of C60 along the nanotubes length from the theoretical continuum model as well as MD simulations. In the theoretical model, C60 is displaced to different locations along the nanotube, and the potential energy of molecule is calculated at each position from the integrals shown in Eq. 5. Since the tube lies between $15 < z < 55$, there is no surface atoms in the left vicinity of fullerene when its position is $z < 15$ and hence the potential energy between fullerene and tube increases. Similar increase in potential energy is observed when fullerene position is $z > 55$. These sudden changes in potential energy act like energy barrier and prevent fullerene to exit from the conical tube surface except at sufficiently higher temperatures.

The variation of the potential energy of C60 has been shown in Fig. 3 as the molecule travels the length of cone-shaped CNT. The potential energy level decreases as C60 moves toward the narrower end of CNT, which confirms the presence of a driving force on the molecule. By decreasing the opening angle from 112.9∘ (Fig. 3a) to 60.0∘ (Fig. 3b), the potential energy level decays to lower values, which is attributed to the increase of contact area between C60 and CNT, at smaller opening angles. It is found that, the fullerene experiences larger energy gradient by decreasing the opening angles (e.g., 19.2° in Fig. 3c), which is equal to 0.28 eV. As a result, the decrease of opening angle leads to the faster transport of C60 along the nanotube length. Due to the increase of potential energy gradient (driving force) on the fullerene at smaller opening angles, we expect to observe more directed movements. The simulation results are also illustrated in Fig. 3a and c by hollow circle. The simulation results are completely compatible with the results obtained from the continuum model (dashed lines). The sudden increase of the potential energy in the results of the continuum model refers to energy level when the molecule is out of the cone-shaped nanotube.

Cone-shaped CNTs with different opening angles

In this section, we aim to study the effect of opening angles of CNTs, on the motion of fullerene molecules inside the nanotubes. The opening angles of imaginary cones are considered 112.9, 60.0, and 19.2 degrees. The radius of these CNTs decreases linearly, along their axes such as $76.6\,\text{Å} \rightarrow 10.0\,\text{Å}$, $50.0\,\text{Å} \rightarrow 10.0\,\text{Å}$, and $23.3\,\text{Å} \rightarrow 10.0\,\text{Å}$. The slant length in different carbon nanotubes is equal to 80 Å. In Fig. 4, the snapshots of the motion of C60 fullerenes are demonstrated inside the cone-like CNTs from the top view. As we observe in this figure, the molecules experience directed motions to the narrower end of the nanotubes. However, the rectilinearity of the movements depends on the opening angles of the CNTs. According to Fig. 4, at larger opening angles (e.g., 112.9°), although the molecule moves toward the narrower end of CNT, it does not walk on a straight path. As we decrease the cone angle to lower values (e.g., 60.0°), the C60 shows more directed motion to the end of CNT. The translocation time also lessens by decreasing the opening angle of CNTs. At the opening angle of 112.9°, the fullerene travels the length of CNT in 560 picoseconds; while, in case of $\alpha = 60.0°$, C60 passes the same length in 73 picoseconds. It seems that, by decreasing the opening angle, the driving force on the fullerene increases. The validity of the last claim would be examined by the analysis of potential energy.

The reproducibility of the directed motion has been examined, by performing the simulations with different initial conditions of C60. The simulations have been repeated five times, while the initial coordinates of fullerenes are similar, but the distribution of the initial velocity is different in each simulation. Figure 5 illustrates the trajectories of the motion of fullerene molecules inside the cone-like CNTs, from the top view. Based on the
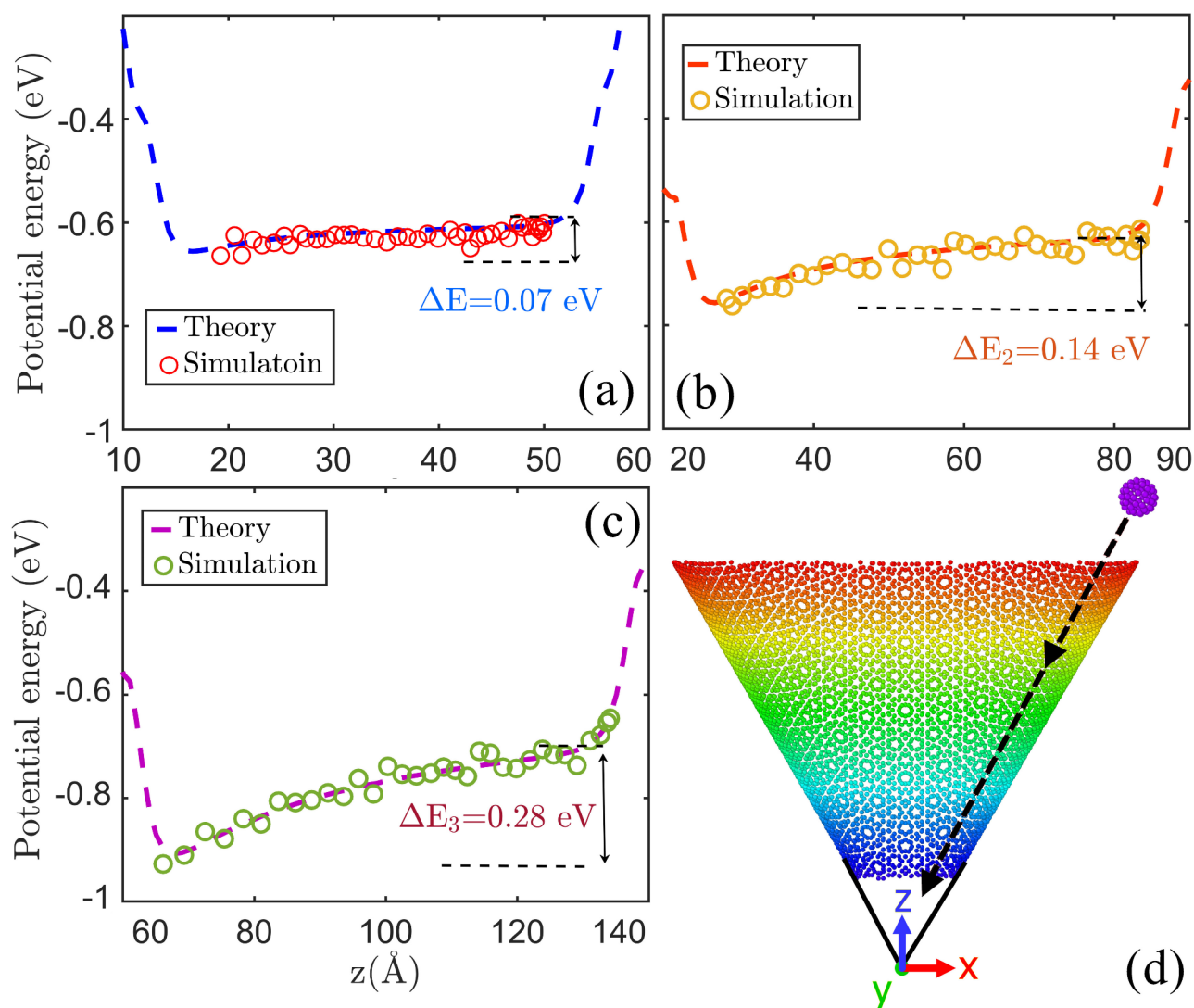
Fig. 3. The potential energy of C60 as a function molecule's height. C60 travels the length of cone-shaped CNT, and it is located in equilibrium distance to the CNT wall. The opening angles of nanotubes are (a) 112.9∘, (b) 60.0∘, and (c) 19.2∘. The variation of the potential energy has been obtained by presenting a continuum model and numerical simulations. (d) The trajectory of the displacements of C60 has been shown inside the nanotube.

results of the simulations, at each opening angle of CNT, the fullerene prefers to move toward the narrower end of the nanotube. When the opening angle of the nanotube is 112.9° (Fig. 5a), the motion of C60 is almost diffusive; however, it reaches the narrower end of nanotube during the simulation. As the opening angle decreases to 60.0° and 19.2° (Fig. 5b and c), we observe more directed movements, and the fullerene travels the length of CNT in more straight paths. In case of $\alpha = 19.2°$, in most of the simulations, the molecule shows spiral motions as it approaches the end of nanotube (Fig. 5c). According to the analysis of potential energy (Fig. 3), the driving force on the C60 molecule increases by decreasing the opening angle of the cone-shaped nanotubes. Since a larger driving force is acting on the C60 at smaller opening angles, the molecule is less affected by the random forces of the thermal fluctuations. As a result, the fullerene molecule maintains the direction of the initial velocity, particularly in the azimuth direction. The preserved direction of the azimuth velocity leads to the observation of spiral motions at smaller opening angles.

The average trajectory of the motions was obtained for each opening angle (black curves in Fig. 5). At different opening angles of cone-shaped CNTs, the average trajectories almost show the directional transport of C60 molecules to the narrower end of nanotubes. However, the standard deviations are larger at different points for CNTs with larger opening angles (e.g., $\alpha = 112.9°$). On the other hand, the standard deviation decreases at smaller opening angles such as $19.2°$, especially in the direction of y-axis. As a result, the fullerene experiences more directional movements inside the cone-shaped CNTs with smaller opening angles.

Using the following equation, mean square displacements has been measured for the directed motions, at different opening angles of CNTs.
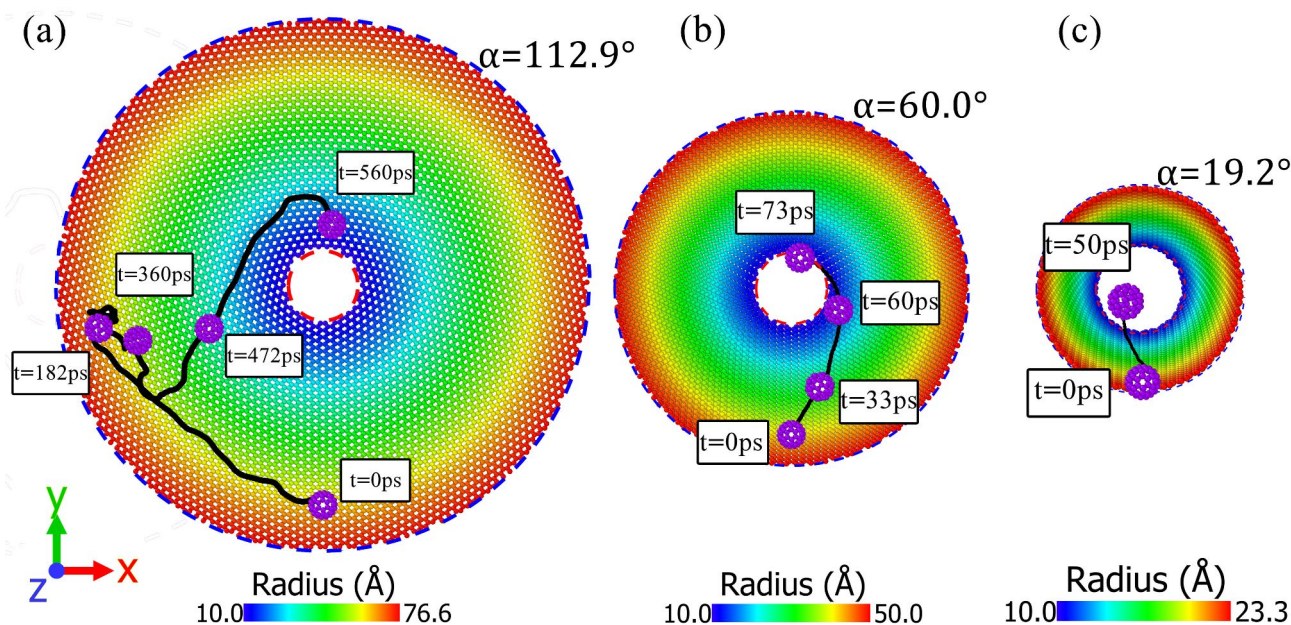
Fig. 4. Snapshots of the motion of C60 inside the cone-like nanotubes with the opening angles of 112.9, 60.0 and 19.2 degrees. The color bars indicate the variation of the nanotubes radius.
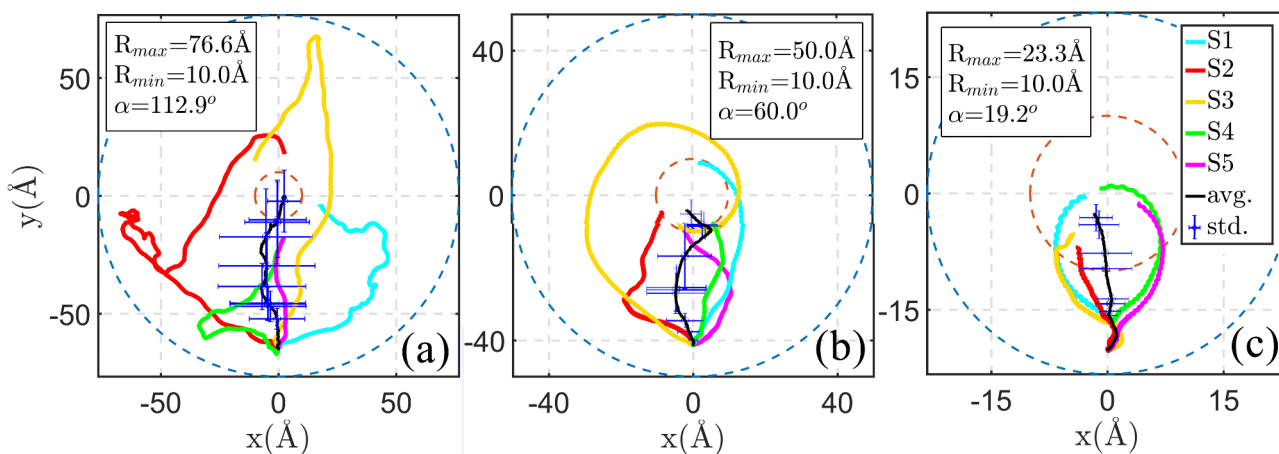

Fig. 5. Trajectories of the motion of fullerene on the CNTs with the opening angles of (a) 112.9, (b) 60.0 and (c) 19.2 degrees. At each opening angle of CNT, the distribution of the initial velocity is different on the fullerene atoms.

$$MSD = \left\langle \left(z\left(t\right) - z\left(0\right)\right)^2 \right\rangle = 2Dt^{\beta} \tag{7}$$

In Eq. 7, $z\left(t\right)$ and $z\left(0\right)$ are the coordinates of the C60 in the direction of nanotube length at time t and 0, respectively. The angle brackets in this equation also refer to the ensemble averaging, which is conducted by averaging the square displacements over five simulations with different seed numbers. Figure 6 illustrates the MSDs of the directed movements of fullerene as the functions of simulation time. As we decrease the opening angles of CNTs, the MSD of the directed motion grows faster with time.

The mean square displacements is related to the diffusion coefficient (D) through the power-law relation presented in Eq. 7. In this equation, the diffusion regime is determined by the β parameter, which is named as anomaly parameter. Table 1 indicates that the diffusion coefficient of the directed motion increases by decreasing the opening angle of cone-like nanotubes. The larger diffusion coefficient of C60 is related to the growth of driving force at smaller opening angles (previously concluded from Fig. 3). According to Table 1, since the anomaly parameter is larger than 1, the fullerene motion follows a super-diffusive regime, at different angles of cone-like nanotubes. However, the anomaly parameter relatively finds lower values at larger opening angles of the CNTs.
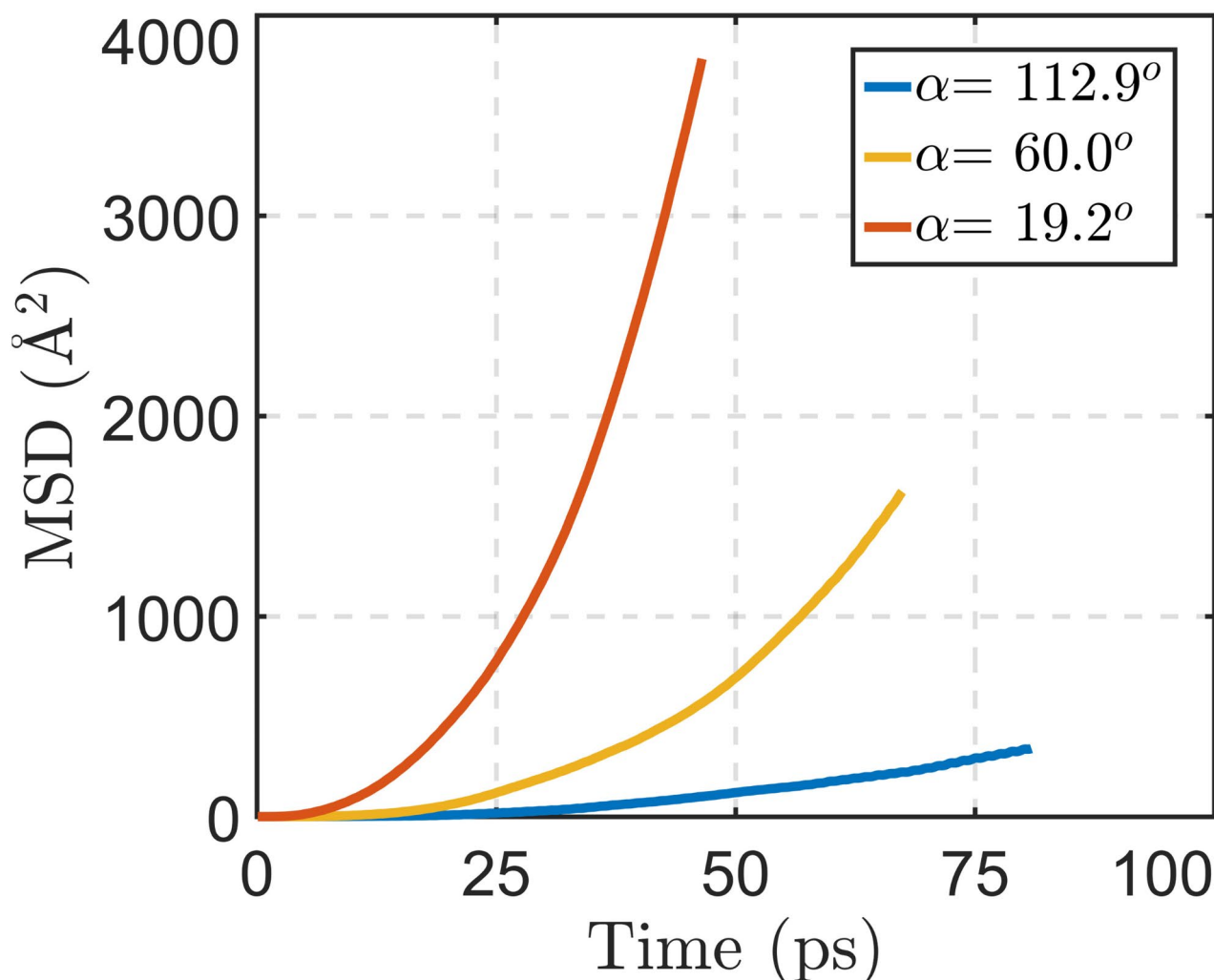
Fig. 6. Mean square displacements of fullerene have been obtained during the motion inside the CNTs with different opening angles.

α (degree)	D(Å²/ps)	β
19.2	0.055	2.721
60.0	0.016	2.567
112.9	0.007	2.295

Table 1. Diffusion coefficients and anomaly parameters of the directed motion C60 inside the nanotubes with different opening angles.

Effect of average radius on the directed transportation

In this section, we evaluate the effect of average radius on the directed movements of fullerene. For this purpose, three types of nanotubes have been chosen, which are similar in opening angle, but vary in the average radius. The opening angle of three nanotubes is 38.9°, while the radius of CNTs linearly changes from 7.9 Å to 34.5 Å, from 34.5 Å to 61.2 Å and from 61.2 Å to 87.9 Å. In these nanotubes, the average values of the radius are 21.2 Å, 47.85 Å, and 74.55 Å, respectively. Figure 7 demonstrates the trajectories of the motion fullerene inside these nanotubes, which have the same opening angle of 38.9° and the same slant length of 80 Å, but they are different in average radius. At the average radius of 21.2 Å (Fig. 7a), the fullerene travels the length of CNT in a more directed path. By increasing the average radius to 47.85 and 74.55 Å (Fig. 7b and c), we observe more random movements in the trajectories of the fullerene. As a result, the increase of average radius in cone-like nanotubes hinders the directed motion of molecules inside the tube. This result seems reasonable, because in the case of a very large average radius, the fullerene interacts with a lower number of CNTs atoms, and it hardly senses

8
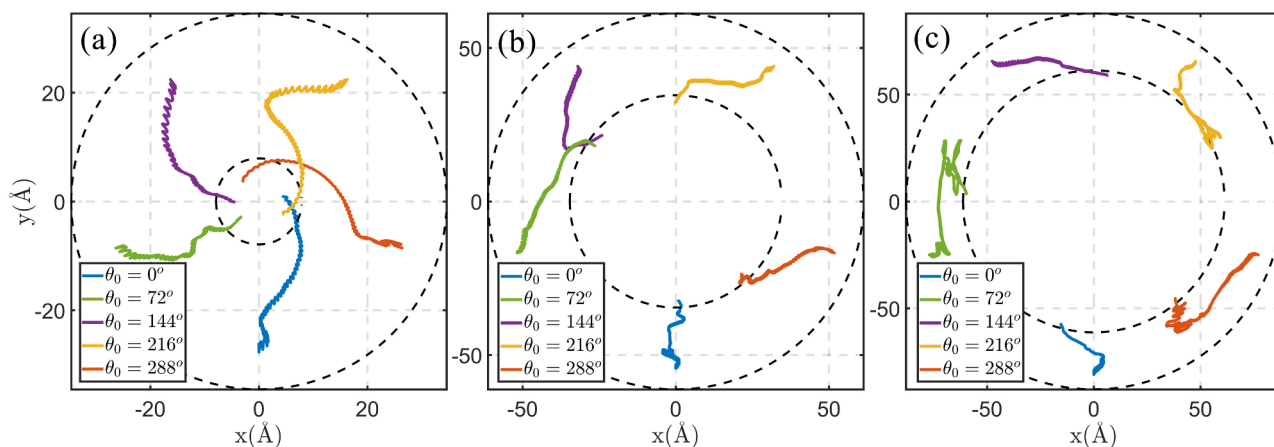
Fig. 7. Trajectories of the motion of fullerene in cone-like nanotubes with similar opening angle of 38.9 degrees. The radius of nanotubes linearly changes as (a) 7.9 Å → 34.5 Å, (b) 34.5 Å → 61.2 Å and (c) 61.2 Å → 87.9 Å.
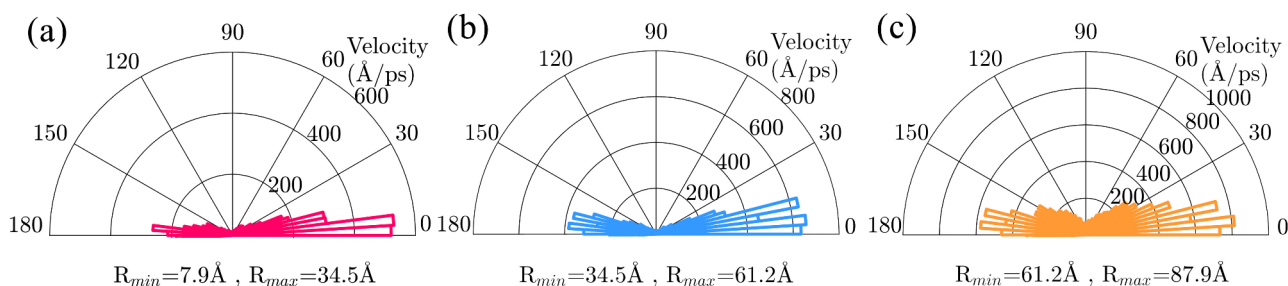
Fig. 8. Distribution of the horizontal velocity of C60, in different angles relative to the direction of $-\hat{r}$, when the radius of nanotubes changes as (a) 7.9 Å → 34.5 Å, (b) 34.5 Å → 61.2 Å and (c) 61.2 Å → 87.9 Å. The results are extracted from five simulations with different initial conditions of C60.

the curvature of the nanotube. On the other hand, when the radius of CNT is small enough (compared with molecule size), the directed transport is better observed along the cone-like nanotube.

To better quantify the directionality of the motion, we calculated the distribution of the fullerene horizontal velocity relative to a unit vector that perpendicular pints to the nanotube axis (named as $\hat{n}$). At each point such as (x_0, y_0, z_0), the $\hat{n}$ vector is defined as,

$$\hat{n} = -\hat{r} = -(x_0, y_0, 0)/\| (x_0, y_0, 0) \| \tag{8}$$

where, $\hat{r}$ is the normal radial vector in the cylindrical coordinate system, and the brackets calculate the length of the vector. In case of a rectilinear motion to the apex of a cone-like CNT, the horizontal velocity of fullerene (i.e., $(v_x, v_y, 0)$) is completely in the direction of the $\hat{n}$, at each step of the simulation. The distribution of the C60 horizontal velocity around the $\hat{n}$ has been obtained for different average radii of the CNT (Fig. 8). It should be mentioned that, analogous to the previous analysis in Fig. 7, the opening angle is similar in all of the nanotubes (38.9 degrees), and they are repeated five times to ensure the obtained results.

At the average radius of 21.2 Å (Fig. 8a), the horizontal velocity is mostly distributed in the directions around 0 degree, which means that C60 moves in the direction of the $\hat{n}$ most of the time. Consequently, the molecule almost experiences a directed movement toward the apex of the cone-like CNT, when the average radius is 21.2 Å. At larger average radius of nanotube such as 47.85 Å, and 74.55 Å (Fig. 8b and c), we observe the growth of velocity distribution in the directions other than the direction of $\hat{n}$. However, a larger portion of the velocity is still distributed around 0 degree, which implies the directed movement of the molecule. As a result, in case of larger average radius of CNT, the fullerene spends more time moving in the random directions, but it still prefers to reach the narrower end of the nanotube. The last results are in agreement with the trajectories of the motion, which have already been shown in Fig. 7.
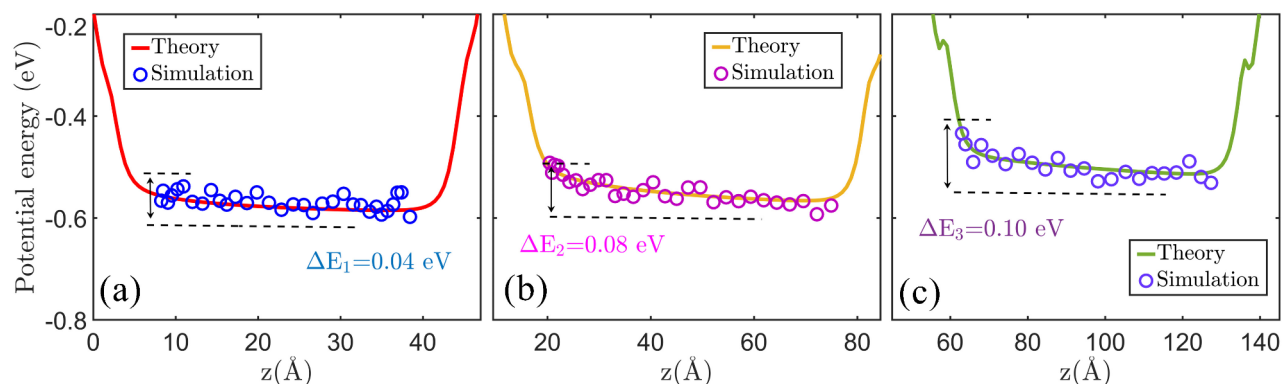
Fig. 9. Potential energy of C60 when it moves outside the cone-shaped nanotubes with the opening angles of (a) 112.9°, (b)60.0° and (c) 19.2°. The variation of the potential energy was obtained from the continuum model as well as the numerical simulations.
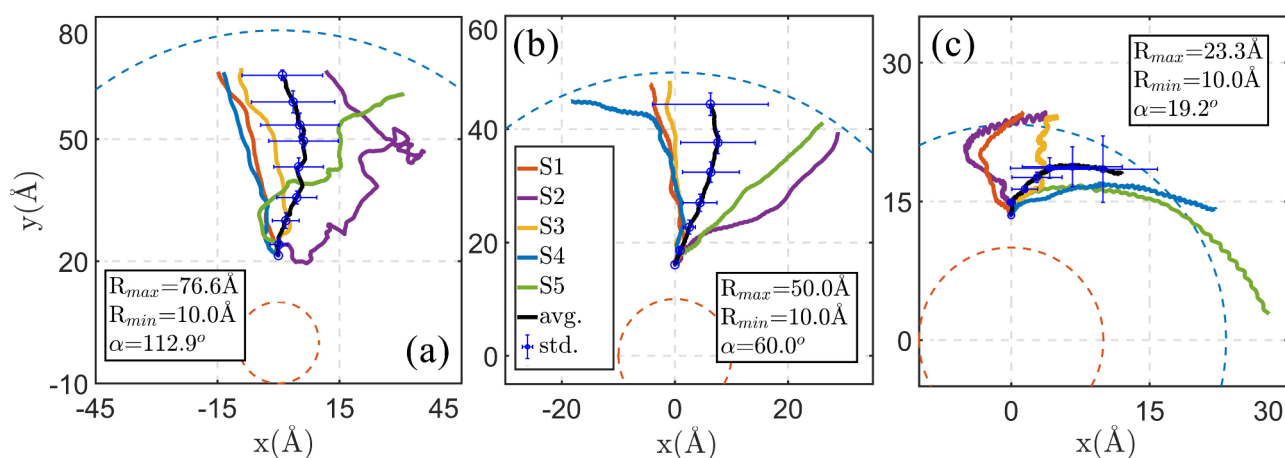
Fig. 10. Trajectories of the motion of C60 outside the cone-like carbon nanotubes with the opening angles of (a) 112.9°, (b)60.0° and (c) 19.2°. The averages and standard deviations of the trajectories are demonstrated in the figure.

Moving outside the cone-shaped nanotubes

Using carbon nanotubes as the tips of the atomic force microscope[49] leads to the higher imaging resolution[50] as well as, the precise manipulation of molecules at nano-scale dimensions[51]. As a result, controlling the motion of adsorbed molecules outside the CNT is of interest in the field of nano-manipulation.

The variation of the potential energy of C60 molecule has been evaluated using the continuum model present in Sect. 3.1, as well as the numerical simulations. According to Fig. 9, the potential energy of the molecule decreases as it moves toward the wider end of the cone-shaped CNT. Compared to the case where C60 moves inside the nanotube (Fig. 3), the direction of the energy gradient is different. The molecule prefers to move from the narrower end of CNT to wider regions, because the molecule has lower potential energy on wider regions. This conclusion seems reasonable, because when the fullerene is on the wider end of the nanotube there is larger area of CNT under the C60 and the fullerene interacts with more CNTs atoms. The fullerene experiences a larger energy gradient when it moves outside the cone-shaped nanotubes with smaller opening angles. For example, at the opening angle of 19.2° (Fig. 9c) the potential energy of C60 changes by 0.1 eV from narrower end to wider side of the CNT. The energy gradients in Fig. 9 are smaller than the ones observed when C60 was inside the nanotube (Fig. 3). It should be mentioned that, as we observe in Fig. 9, the results of the theoretical model are in agreement with the variations of the energy recorded from the simulations.

The trajectories of the motion of C60 has been captured during the motion outside the cone-shaped nanotubes with different opening angles. As we observe in Fig. 10, the trajectories of the motion confirm the migration of fullerene molecule from the parts with smaller radius to the regions with larger radius. To examine the repeatability of the result, five simulations have been performed by changing seed number. At the opening angles of 112.9° and 60.0° (Fig. 10a and b), the average path of the motion is more straight. While at the opening angle of 19.2°, since the molecule rotates around the CNT, the average trajectory indicates an almost spiral path.
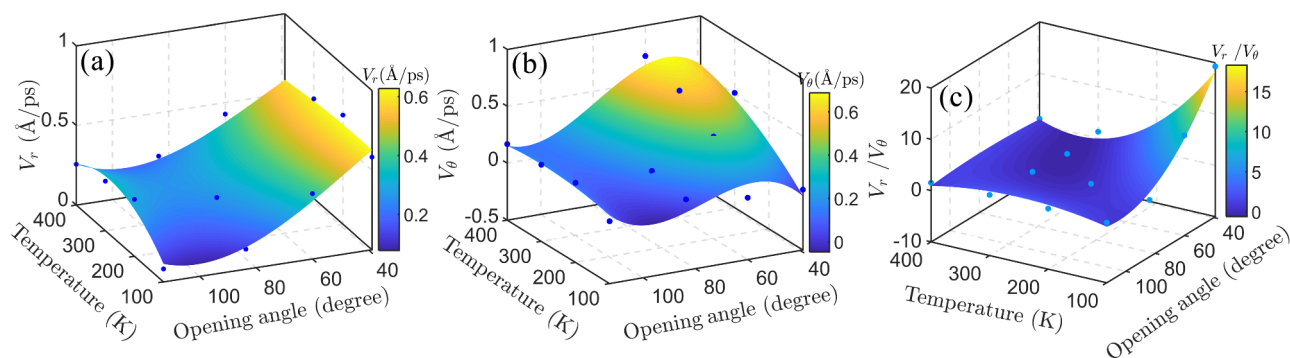
Directed transportation at different temperatures

To understand the effect of temperature on the directionality of motion inside the cone-like nanotubes, the simulations have been conducted at the temperature range of 100 to 400 K. At each temperature, we calculate different parameters such v_r and v_θ, which are the average values of radial and angular speeds of fullerene, in the cylindrical coordinate system. In the rectilinear transport of C60 toward the narrower end of CNT, the speed of molecule is in radial direction, while the angular speed has a negligible share. As a result, the v_r/v_θ ratio has also been calculated, which is another criterion to understand the directionality of the fullerene motion.

According to Fig. 11a, the radial speed is more affected by the opening angle of CNTs, rather than the temperature of the environment. At the opening angle of 112.9°, the radial speed increases by raising the temperature, which is related to the growth of thermal energy at higher temperatures. However, the increase of radial speed with the temperature is not observable clearly at smaller opening angles of CNTs. Figure 11b demonstrates the variation of angular speed at different temperatures, and opening angles of nanotubes. As the temperature rises, the angular speed of fullerene also increases, especially at smaller opening angles such as 38.9°. The angular speed growth refers to the non-directional movements of the C60 molecule at higher temperatures. The ratio of radial speed to angular one (v_r/v_θ) indicates the proper conditions for achieving directional motion inside the cone-like CNTs. According to Fig. 11c, the v_r/v_θ ratio considerably increases as the opening angle of nanotube decreases, and when the temperature of the system is lower. The last conclusion is consistent with the trajectories of motion and potential energy gradients in Figs. 3 and 5, respectively. At smaller opening angle of CNT, larger driving force is acting on the C60, which leads to a directional movement inside the cone-like nanotube. Moreover, as we increase the temperature, the thermal fluctuations hinder the directed transport of fullerene and the molecule experiences non-directional movements in the random directions.

Previous investigations on the one-dimensional directed transport of nanomaterials can be categorized to different groups. In some of the studies the one-dimensional movements occur on the surface. It is possible to steer the motion of materials on the surface, by applying some modifications on the substrates. Nemati et al.[52] demonstrated the restricted movements of fullerene molecule along the edge of the atomic steps on the gold surface. Using hybrid substrates is another method to restrict the lateral motion of molecules on the surface[53]. According to the previous investigations, on the gold-silver hybrid substrate, the adsorbed molecules prefers to move on gold regions due to the lower potential energy of molecule on this area[53]. Using the atomic vacancies on the substrate is another technique which has been proposed to constrain the surface motion in one-dimension[54]. Although these modifications of the substrates help to restrict the surface motion in one-dimension, the direction of the movements is not under control in these methods. In some of the previous works, an external agent has been employed for achieving directional motions. The electric field of the scanning electron microscope is able to manipulate the particles on the surface in a desired direction[55]. This type of manipulation is commonly implemented in the experimental investigations[56]. By applying transverse vibration on the graphene nanoribbon, Chen et al.[57] demonstrated that the adsorbed nanoparticle moves away from the fluctuating regions, a phenomenon named as fluctuotaxis. The difference in atomic fluctuations of the substrate behind and ahead of the nanoparticle gives rise to a driving force acting on the adsorbed particle.

Another group of investigations utilize carbon nanotubes as a track for the one-dimensional directed transportation. The nanotubes subjected to temperature gradient can direct the encapsulated nanoparticles toward the regions with lower temperature[58], because the particle finds lower free energy on this area[59]. The directed transportation of nanomaterials on the CNTs is also available by passing the electric current through the carbon nanotubes[60]. According to the electromigration phenomenon, the direction of motion is controllable by changing the current direction. The directed motions caused by electromigration and temperature gradient are utilized to fabricate nanomachines based on carbon nanotubes[5,6]. Directed transport of materials along the carbon nanotubes is also achievable by performing some modifications on the structure of nanotubes. As previously mentioned, the spiral-shaped nanotubes are able to direct the motion of encapsulated nano-objects[33]. The curvature gradient in these nanotubes leads to a driving force toward the areas with lower curvatures. In this study, we showed that the conical structure of the nanotubes steers the motion of molecules located on the

Fig. 11. The average values of (a) radial and (b) angular speeds of C60 at different temperatures and opening angles of cone-like nanotubes. (c) The ratio of radial to angular speed has been obtained as a criterion for the directional transport of molecule inside the CNTs.

internal and external surfaces of the CNTs. The synthesis of cone-shaped nanotubes is experimentally feasible[61]. Therefore, it is conceivable to put this novel approach for directed transport of nanomaterials into practice.

Conclusions

Directed transport of C60 fullerene has been studied along the cone-like nanotubes, using molecular dynamics simulations. The radius of CNTs decreases linearly as we move along the nanotube length. According to the results of the simulations, the fullerene experiences directed movements toward the narrower end of the CNTs. The potential energy of the molecule is lower at the narrower end of the nanotube, which is due to the increase of interactions between the C60 molecule and the CNT surface.

Different opening angles were chosen for the nanotubes including 112.9, 60.0, and 19.2 degrees. The trajectories of the motion of fullerene revealed that, the C60 molecule has more directional movement inside the CNTs with smaller opening angles (e.g., 19.2°). To understand the reason for this observation, variations of the potential energy were obtained at different opening angles of CNTs. Based on the results of the simulations, by decreasing the opening angle of nanotube, the driving force on the fullerene becomes larger. At smaller opening angles, the molecule finds a larger potential energy gradient, which leads to the rectilinear motion of C60. Based on the mean square displacement analysis, the fullerene showed larger diffusion coefficients as the opening angle of CNT decreases.

At a constant opening angle, the directionality of the motion was examined at different average radius of CNT. For this purpose, the opening angle of nanotubes was chosen 38.9°, while the radius of CNTs linearly changed as 7.9 Å → 34.5 Å, 34.5 Å → 61.2 Å and 61.2 Å → 87.9 Å. The trajectories of the fullerene motion demonstrated that, the C60 has more diffusive motions inside the nanotubes with larger average radius (e.g. 61.2 Å → 87.9 Å). On the other hand, at smaller average radius of nanotubes (e.g. 7.9 Å → 34.5 Å), the fullerene showed a directed motion toward the narrower end of CNT. The distribution of the horizontal velocity of fullerene also revealed that, when the average radius of CNT is smaller, the directed transport is better achieved along the cone-like nanotube.

The motion of fullerene molecules has been studied outside the cone-like nanotube. The directed transport of C60 was observed in the opposite direction, when the molecule moves outside the CNT. It has been shown that, when the fullerene is located outside the CNT, it has stronger interactions with the parts with larger radius. The fullerene motion inside the cone-like nanotube has been evaluated at the temperature range of 100 to 400 K. The ratio of radial to angular speed (v_r/v_θ ratio) indicated that the C60 molecule has more directed movement, at smaller opening angle of nanotube, and lower temperatures. As we increase the temperature, the thermal fluctuations hinder the directed transport of fullerene and the molecule experiences movements in random directions.

Data availability

The data that support the findings of this study are available on request from the corresponding author.

References

1. Sheikhpour, M. et al. An effective nano drug delivery and combination therapy for the treatment of tuberculosis. *Sci. Rep.* **12**(1), 9591 (2022).
2. Kamazani, F. M., Sotoodehnejad nematalahi, F., Siadat, S. D., Pornour, M. & Sheikhpour, M. A success targeted nano delivery to lung cancer cells with multi-walled carbon nanotubes conjugated to bromocriptine. *Sci. Rep.* **11**(1), 24419 (2021).
3. Chai, Z., Childress, A. & Busnaina, A. A. Directed assembly of nanomaterials for making nanoscale devices and structures: mechanisms and applications. *ACS nano*. **16**(11), 17641–17686 (2022).
4. Wang, J. & Nakano, T. (eds) Collective rotational motion of bio-nanomachines via chemical and physical interactions. GLOBECOM 2022–2022 IEEE Global Communications Conference; : IEEE. (2022).
5. Regan, B., Aloni, S., Ritchie, R., Dahmen, U. & Zettl, A. Carbon nanotubes as nanoscale mass conveyors. *Nature*. **428**(6986), 924–927 (2004).
6. Barreiro, A. et al. Subnanometer motion of cargoes driven by thermal gradients along carbon nanotubes. *Science*. **320**(5877), 775–778 (2008).
7. Miners, S. A., Rance, G. A. & Khlobystov, A. N. Chemical reactions confined within carbon nanotubes. *Chem. Soc. Rev.* **45**(17), 4727–4746 (2016).
8. Eskandari, S., Koltai, J., László, I., Vaezi, M. & Kürti, J. Formation of nanoribbons by carbon atoms confined in a single-walled carbon nanotube—A molecular dynamics study. *J. Chem. Phys.* **158**(22). (2023).
9. Nakanishi, R. et al. Thin single-wall BN-nanotubes formed inside carbon nanotubes. *Sci. Rep.* **3**(1), 1–6 (2013).
10. Kuzmany, H. et al. Well-defined sub-nanometer graphene ribbons synthesized inside carbon nanotubes. *Carbon*. **171**, 221–229 (2021).
11. Khlobystov, A. N. Carbon nanotubes: from nano test tube to nano-reactor. *ACS nano*. **5**(12), 9306–9312 (2011).
12. Terrones, M. Visualizing fullerene chemistry. *Nat. Chem.* **2**(2), 82–83 (2010).
13. Wilson, N. R. & Macpherson, J. V. Carbon nanotube tips for atomic force microscopy. *Nat. Nanotechnol.* **4**(8), 483–491 (2009).
14. Siria, A. & Niguès, A. Electron Beam detection of a nanotube scanning force microscope. *Sci. Rep.* **7**(1), 11595 (2017).
15. Gao, Z. et al. Optical detection of individual ultra-short carbon nanotubes enables their length characterization down to 10 nm. *Sci. Rep.* **5**(1), 17093 (2015).
16. Wei, H. et al. Control of length and spatial functionality of single-wall carbon nanotube AFM nanoprobes. *Chem. Mater.* **20**(8), 2793–2801 (2008).
17. Vaezi, M. Nanomachines Based on Carbon Nanotubes. (2024).
18. Vaezi, M., Pishkenari, H. N. & Nemati, A. Mechanism of the motion of nanovehicles on hexagonal boron-nitride: a molecular dynamics study. *Comput. Mater. Sci.* **207**, 111317 (2022).
19. Vaezi, M., Nejat Pishkenari, H. & Nemati, A. Mechanism of C60 rotation and translation on hexagonal boron-nitride monolayer. *J. Chem. Phys.* **153**(23). (2020).
20. Wang, J. & Manesh, K. M. Motion control at the nanoscale. *Small*. **6**(3), 338–345 (2010).

21. Kianezhad, M., Youzi, M., Vaezi, M. & Pishkenari, H. N. Rectilinear motion of carbon nanotube on gold surface. *Int. J. Mech. Sci.* **217**, 107026 (2022).
22. Zhang, B. et al. Rapid programmable nanodroplet motion on a strain-gradient surface. *Langmuir*. **35**(7), 2865–2870 (2019).
23. Vaezi, M., Nejat Pishkenari, H. & Ejtehadi, M. R. Programmable transport of C60 by straining graphene substrate. *Langmuir*. **39**(12), 4483–4494 (2023).
24. Vaezi, M. & Nejat Pishkenari, H. Toward steering the motion of surface rolling molecular machines by straining graphene substrate. *Sci. Rep.* **13**(1), 20816 (2023).
25. Huang, Y., Zhu, S. & Li, T. Directional transport of molecular mass on graphene by straining. *Extreme Mech. Lett.* **1**, 83–89 (2014).
26. Vaezi, M. Programmable oscillation of C60 inside carbon nanotubes subjected to strain gradient. *J. Appl. Phys.* **134**(23). (2023).
27. Nirmalraj, P., Daly, R., Martin, N. & Thompson, D. Motion of Fullerenes around Topological defects on metals: implications for the Progress of Molecular Scale devices. *ACS Appl. Mater. Interfaces.* **9**(9), 7897–7902 (2017).
28. Youzi, M., Kianezhad, M., Vaezi, M. & Pishkenari, H. N. Motion of nanovehicles on pristine and vacancy-defected silicene: implications for controlled surface motion. *Phys. Chem. Chem. Phys.* **25**(42), 28895–28910 (2023).
29. Kianezhad, M., Youzi, M., Vaezi, M. & Nejat Pishkenari, H. Unidirectional motion of C60-based nanovehicles using hybrid substrates with temperature gradient. *Sci. Rep.* **13**(1), 1100 (2023).
30. Lohrasebi, A., Neek-Amal, M. & Ejtehadi, M. Directed motion of C 60 on a graphene sheet subjected to a temperature gradient. *Phys. Rev. E.* **83**(4), 042601 (2011).
31. Leng, J., Hu, Y. & Chang, T. Nanoscale directional motion by Angustotaxis. *Nanoscale.* **12**(9), 5308–5312 (2020).
32. Legoas, S. et al. Molecular-dynamics simulations of carbon nanotubes as gigahertz oscillators. *Phys. Rev. Lett.* **90**(5), 055504 (2003).
33. Machado, L. D., Bizao, R. A., Pugno, N. M. & Galvão, D. S. Controlling movement at nanoscale: curvature driven mechanotaxis. *Small.* **17**(35), 2100909 (2021).
34. Berkmans, J., Jagannatham, M., Reddy, R. & Haridoss, P. Synthesis of thin bundled single walled carbon nanotubes and nanohorn hybrids by arc discharge technique in open air atmosphere. *Diam. Relat. Mater.* **55**, 12–15 (2015).
35. Chen, I-C. et al. Fabrication of high-aspect-ratio carbon nanocone probes by electron beam induced deposition patterning. *Nanotechnology.* **17**(17), 4322 (2006).
36. Saito, Y. & Arima, T. Growth of cone-shaped carbon material inside the cell lumen by heat treatment of wood charcoal. *J. Wood Sci.* **48**, 451–454 (2002).
37. Shoyama, K. & Würthner, F. Synthesis of a carbon nanocone by cascade annulation. *J. Am. Chem. Soc.* **141**(33), 13008–13012 (2019).
38. Zhu, Z-Z. et al. Rational synthesis of an atomically precise carboncone under mild conditions. *Sci. Adv.* **5**(8), eaaw0982 (2019).
39. Melchor, S., Dobado, J. A. & CoNTub An algorithm for connecting two arbitrary carbon nanotubes. *J. Chem. Inf. Comput. Sci.* **44**(5), 1639–1646 (2004).
40. Baskar, A. V. et al. Self-assembled fullerene nanostructures: synthesis and applications. *Adv. Funct. Mater.* **32**(6), 2106924 (2022).
41. Nosé, S. A unified formulation of the constant temperature molecular dynamics methods. *J. Chem. Phys.* **81**(1), 511–519 (1984).
42. Hoover, W. G. Canonical dynamics: equilibrium phase-space distributions. *Phys. Rev. A.* **31**(3), 1695 (1985).
43. Vaezi, M., Pishkenari, H. N. & Ejtehadi, M. R. Nanocar swarm movement on graphene surfaces. *Phys. Chem. Chem. Phys.* **24**(45), 27759–27771 (2022).
44. Rafii-Tabar, H. Computational modelling of thermo-mechanical and transport properties of carbon nanotubes. *Phys. Rep.* **390**(4–5), 235–452 (2004).
45. Tersoff, J. Modeling solid-state chemistry: interatomic potentials for multicomponent systems. *Phys. Rev. B.* **39**(8), 5566 (1989).
46. Thompson, A. P. et al. LAMMPS-a flexible simulation tool for particle-based materials modeling at the atomic, meso, and continuum scales. *Comput. Phys. Commun.* **271**, 108171 (2022).
47. Lippert, R. A. et al. A common, avoidable source of error in molecular dynamics integrators. *J. Chem. Phys.* **126**(4). (2007).
48. Vaezi, M., Pishkenari, H. N. & Ejtehadi, M. R. Collective movement and thermal stability of fullerene clusters on the graphene layer. *Phys. Chem. Chem. Phys.* **24**(19), 11770–11781 (2022).
49. Cheng, B. et al. Controlled growth of a single carbon nanotube on an AFM probe. *Microsystems Nanoengineering.* **7**(1), 80 (2021).
50. Cheung, C. L., Hafner, J. H. & Lieber, C. M. Carbon nanotube atomic force microscopy tips: Direct growth by chemical vapor deposition and application to high-resolution imaging. Proceedings of the National Academy of Sciences. ;97(8):3809-13. (2000).
51. Firouzi, M. M., Pishkenari, H. N., Mahboobi, S. & Meghdari, A. Manipulation of biomolecules: a molecular dynamics study. *Curr. Appl. Phys.* **14**(9), 1216–1227 (2014).
52. Nemati, A., Pishkenari, H. N., Meghdari, A. & Sohrabpour, S. Directing the diffusive motion of fullerene-based nanocars using nonplanar gold surfaces. *Phys. Chem. Chem. Phys.* **20**(1), 332–344 (2018).
53. Nemati, A., Nejat Pishkenari, H., Meghdari, A. & Ge, S. S. Controlling the diffusive motion of fullerene-wheeled nanocars utilizing a hybrid substrate. *J. Phys. Chem. C.* **123**(42), 26018–26030 (2019).
54. Nemati, A., Nejat Pishkenari, H., Meghdari, A. & Ge, S. S. Influence of vacancies and grain boundaries on the diffusive motion of surface rolling molecules. *J. Phys. Chem. C.* **124**(30), 16629–16643 (2020).
55. Akimov, A. V. & Kolomeisky, A. B. Unidirectional rolling motion of nanocars induced by electric field. *J. Phys. Chem. C.* **116**(42), 22595–22601 (2012).
56. Shirai, Y., Osgood, A. J., Zhao, Y., Kelly, K. F. & Tour, J. M. Directional control in thermally driven single-molecule nanocars. *Nano Lett.* **5**(11), 2330–2334 (2005).
57. Chen, Y. et al. Fluctuotaxis: Nanoscale directional motion away from regions of fluctuation. *Proc. Natl. Acad. Sci.* **120**(31), e2220500120 (2023).
58. Wei, N., Wang, H-Q. & Zheng, J-C. Nanoparticle manipulation by thermal gradient. *Nanoscale Res. Lett.* **7**, 1–9 (2012).
59. Lohrasebi, A., Neek-Amal, M. & Ejtehadi, M. Directed motion of C 60 on a graphene sheet subjected to a temperature gradient. *Phys. Rev. E—Statistical Nonlinear Soft Matter Phys.* **83**(4), 042601 (2011).
60. Kulshrestha, N., Misra, A. & Misra, D. Electrical transport and electromigration studies on nickel encapsulated carbon nanotubes: possible future interconnects. *Nanotechnology.* **24**(18), 185201 (2013).
61. Zhang, Q. et al. The synthesis of conical carbon. *Small Methods.* **5**(3), 2001086 (2021).

Author contributions

M.V.: performing simulations, writing manuscript, preparing figures, and providing discussion. H.N.P.: supervision, editing the manuscript, data analysis, providing discussions, proposing the idea of the project.

Declarations

Competing interests

The authors declare no competing interests.

Additional information

Correspondence and requests for materials should be addressed to H.N.P.

Reprints and permissions information is available at www.nature.com/reprints.

Publisher's note Springer Nature remains neutral with regard to jurisdictional claims in published maps and institutional affiliations.